J Solid State Electrochem (2011) 15:1997–2004
DOI 10.1007/s10008-010-1226-2

ORIGINAL PAPER

CO_2 corrosion inhibition of X-70 pipeline steel by carboxyamido imidazoline

D. M. Ortega-Sotelo · J. G. Gonzalez-Rodriguez · M. A. Neri-Flores · M. Casales · L. Martinez · A. Martinez-Villafañe

Received: 20 August 2010 / Revised: 18 October 2010 / Accepted: 20 October 2010 / Published online: 3 November 2010

Abstract The corrosion inhibition of X-70 pipeline steel in saltwater saturated with CO_2 at 50 °C with carboxyamido imidazoline has been evaluated by using electrochemical techniques. Techniques included polarization curves, linear polarization resistance, electrochemical impedance, and electrochemical noise measurements. Inhibitor concentrations were 0, 1.6×10^{-5}, 3.32×10^{-5}, 8.1×10^{-5}, 1.6×10^{-4}, and 3.32×10^{-4} mol l^{-1}. All techniques showed that the best corrosion inhibition was obtained by adding 8.1×10^{-5} mol l^{-1} of carboxyamido imidazoline. For inhibitor concentrations higher than 8.1×10^{-5} mol l^{-1} a desorption process occurs, and an explanation has been given for this phenomenon.

Keywords X-70 steel · CO_2 corrosion · Electrochemical noise

D. M. Ortega-Sotelo · M. A. Neri-Flores · A. Martinez-Villafañe
Centro de Investigaciones en Materiales Avanzados,
Miguel de Cervantes 120, Complejo Ind.,
Chihuahua, Chihuahua, Mexico

J. G. Gonzalez-Rodriguez (✉)
UAEM-CIICAp,
Av. Universidad 1001, Col. Chamilpa,
6225 Cuernavaca, Morelos, Mexico
e-mail: ggonzalez@uaem.mx

M. Casales · L. Martinez
Universidad Nacional Autonoma de Mexico,
Instituto de Ciencias Fisicas,
Av. Universidad s/n, Col. Chamilpa,
6225 Cuernavaca, Morelos, Mexico

L. Martinez
Corrosión y Proteccion Ingenieria SC,
Rio Nazas 6,
CP62290 Cuernavaca, Morelos, Mexico

Introduction

In remote and offshore oil sites, the product from the wells is transported as a mixture of oil, saltwater, and natural gas. Carbon dioxide (CO_2) in the natural gas dissolves in saltwater and results in the formation of a weak carbonic acid often causing severe corrosion in carbon steel pipelines [1, 2]. Corrosion failures, the majority of which are related to CO_2 corrosion [3–6], have been reported to account for some 25% of all safety incidents, 2.8% turnover, 2.2% tangible asset, 8.5% increase on capital expenditure, 5% of lost/deferred production, and 11.5% increase to the lifting costs. The industry continues to lean heavily on the extended use of carbon and low alloy steels, which are readily available in the required volumes and are able to meet many of the mechanical, structural, fabrication, and cost requirements. However, a key issue for their effective use is their poor general and CO_2 corrosion performance. Given the conditions associated with the oil and gas production and transportation, corrosion must always be seen as a potential risk.

For the corrosion control of offshore wet gas pipelines several options are available. The use of corrosion resistant alloys (CRAs) is a relatively new sound solution, although the costs of materials and the added laying time make this alternative unattractive for long distance, large diameter pipelines. The use of low-carbon micro alloyed steels for transportation of wet, corrosive gas offers potential savings over more expensive alternatives, such as the use of CRAs or gas drying, but with a higher risk. However, the use of micro alloyed steels could involve high operating costs due to inhibition practices, inspection, and monitoring.

The use of organic corrosion inhibitors is the most effective way of protecting internal corrosion of carbon steel pipelines for oil product transportation [7–14].

Nitrogen-based organic surfactants, such as imidazolines or their salts have been used successfully as corrosion inhibitors in the oil and gas industries even without an understanding of the inhibition mechanism. For instance, Rodriguez-Valdez et al. [7] have evaluated hydroxyethyl, aminoethyl, and amidoethyl imidazolines; Liu et al. [8] used 2-undecyl-1-aminoethyl imidazoline and 2-undecyl-1-aminoethyl-1-hydroxyethyl quaternary imidazoline; Okafor et al. [9] used 2-undecyl-1-ethylamino imidazoline; Liu et al. [10] evaluated an aminoethyl imidazoline; and Zhang et al. [11] evaluated a hydroxyethyl imidazoline and an imidazoline derivative synthesized from oleic acid, diethylene-triamine, and thiourea.

Most of the above cited works have shown that when an organic inhibitor contains both C and N atoms, the inhibitor efficiency increases considerably. Carboxyamido imidazoline is a five-member ring organic inhibitor containing nitrogen elements, a C-14 saturated hydrophobic head group and a pendant, hydrophilic carboxyamido group attached to one of the nitrogen atoms, and it is thought that it could be a highly efficient CO_2 corrosion inhibitor.

Extensive investigation on field experience with the operation of gas pipelines in corrosive service involving CO_2 corrosion exists in literature [7–16]. With the technology nowadays, corrosion control systems with 100% efficiency can be designed and constructed. The cost of this approach, however, can be cost prohibited and it needs to be balanced against a reduction of corrosion risks. In most cases, pipeline design is based on a value of 95% corrosion control as the maximum achievable following normal equipment and operating procedures.

From these investigations, it has been demonstrated that plain carbon steel pipelines can be safely operated in very corrosive service conditions if the corrosion control system is properly designed and implemented. However, most of these works have been carried out by using standard techniques such as polarization curves, electrochemical impedance spectroscopy (EIS), and linear polarization resistance (LPR) measurements. A few works have been conducted by using electrochemical noise (EN) measurements [17–19]. Moreover, EN measurements have also been successfully applied to the study of corrosion inhibitors performance [17–19]. These measurements are made without any external perturbation of the system and provide information of the actual system being studied with little possibility of artifacts due to the measurement technique.

EN technique involves the estimation of the electrochemical noise resistance, R_n, which is calculated as the standard deviation of potential, σ_v, divided by the standard deviation of current σ_i,

$$R_n = \sigma_v/\sigma_i \quad (1)$$

where R_n can be taken as the linear polarization resistance, R_p in the Stern-Geary equation:

$$I_{corr} = (b_a b_c)/\left[2.3(b_a + b_c)R_p\right] \quad (2)$$

and thus, inversely proportional to the corrosion rate, I_{corr}, but with the necessary condition that trend removal is applied over an average baseline as previously established by Tan et al. [19]. It has been shown that the noise signal contains information about the dynamics that occur on the surface of the electrode and gives information about the type of corrosion that is occurring, either uniform or localized.

The goal of this work is to study the effectiveness and electrochemical behavior of a newly developed high strength pipeline steel in saltwater saturated with carbon dioxide (CO_2) with the addition of carboxyamido imidazoline as corrosion inhibitor by using standard electrochemical techniques, including electrochemical noise measurements

Experimental procedure

Material

The chemical composition (wt.%) of X-70 micro alloyed steel used was 0.044 C, 0.271 Si, 1.69 Mn, 0.0091 P, 0.0103 Cr, 0.240 Ni, 0.0010 V, 0.014 Ti, 0.2170 Cu, 0.25 Mo, 0.0310 Al, 0.0001 B, 0.0554 Nb, 0.0070 Sn, 0.055 As, 0.0018 Pb, 0.0037 Sb, 0.0016 Ca, 0.0040 N, and balance Fe. Specimens had cut in cubes 1.0 cm long, encapsulated in epoxy resin, abraded with 600 grade emery paper, washed, and degreased with acetone.

Testing solution

Inhibitor used in this work was a commercial carboxyamido imidazoline with a molecular structure as shown on Fig. 1, which is composed of a five-member ring containing nitrogen elements, a C-14 saturated hydrophobic head group and a pendant, hydrophilic carboxyamido group attached to one of the nitrogen atoms. Inhibitor was

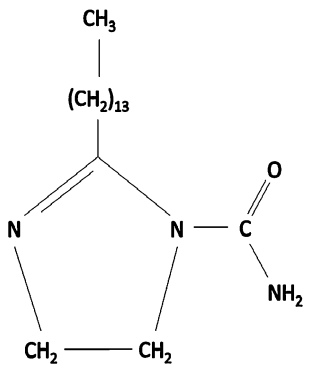

Fig. 1 Molecular structure of carboxyamido imidazoline

dissolved in 100 ml pure 2-propanol. The concentrations of the inhibitor used in this work were 0, 1.6×10^{-5}, 3.23×10^{-5}, 8.1×10^{-5}, 1.6×10^{-4}, and 3.23×10^{-4} mol l^{-1} and the temperature kept at 50 °C. Testing solution consisted of 3% NaCl solution, heated, de-aerated by purging with CO_2 gas during 2 h prior the experiment, and kept bubbling throughout the experiment. Inhibitor was added 2 h after pre-corroding the specimens in the CO_2-containing solution, starting the measurements 1 h later.

Electrochemical measurements

Employed electrochemical techniques included potentiodynamic polarization curves, linear polarization resistance, electrochemical impedance spectroscopy, and electrochemical noise measurements, in both current and voltage. Measurements were obtained by using a conventional three electrodes glass cell with two graphite electrodes symmetrically distributed and a saturated calomel electrode (SCE) as reference with a Lugging capillary bridge. Polarization curves were recorded at a constant sweep rate of 1 mV s^{-1} at the interval from −300 to +300 mV_{SCE} with respect to the open circuit potential, E_{corr}. This scan rate is the commonly used in most of the revised literature [8–15].

From the measured corrosion current density values, I_{corr}, the inhibitor efficiency,η, was calculated by using the relationship:

$$\eta(\%) = \left[\left(I^0{}_{corr} - I_{corr}\right)/I^0{}_{corr}\right] \times 100 \qquad (3)$$

where $I_{corr}{}^0$ and I_{corr} are the uninhibited and inhibited corrosion current density values, respectively. LPR measurements were carried out by polarizing the specimen from +10 to −10 mV_{SCE} with respect to E_{corr}, at a scanning rate of 1 mV s^{-1} every 20 min during 24 h. EIS tests were carried out at the E_{corr} value by using a signal with an amplitude of 10 mV_{SCE} and a frequency interval of 0.1 Hz–30 kHz. An ACM potentiostat controlled by a desk top computer was used for the LPR tests and polarization curves, whereas for the EIS measurements, a model PC4 300 Gamry potentiostat was used.

EN measurements in both current and potential were recorded by using two identical working electrodes and a reference electrode (SCE). Both working electrodes had an exposed area of 1.0 cm^2. EN measurements were made by recording simultaneously the potential and current fluctuations at a sampling rate of 1 point per second during a period of 1,024 s. The noise in current was measured between the two identical working electrodes, whereas the noise in potential was measured versus a SCE electrode. A fully automated zero resistance ammeter from ACM instruments was used in this case. Results are presented without removing the baseline current, instead removal of the DC trend from the raw noise data was performed; to accomplish this, a square fitting method was used. Finally, the noise resistance, R_n, was then calculated as the ratio of the potential noise standard deviation, σ_v over the current noise standard deviation, σ_i.

Results and discussion

Figure 2 shows the effect of carboxyamido imidazoline concentration on the polarization curves of X-70 pipeline steel in the CO_2-saturated 3% NaCl solution at 50 °C. The anodic current density decreases as the inhibitor concentration increases, reaching a lowest value with the addition of 8.1×10^{-5} mol l^{-1}; with a further increase in the carboxyamido imidazoline concentration, the anodic current density increases again. On the other hand, as soon as the inhibitor is added, the cathodic current density decreases; however, its value remained constant regardless the carboxyamido imidazoline concentration. Thus, polarization curves indicate that the corrosion process in presence of inhibitor is under cathodic control and that carboxyamido imidazoline acts as an anodic type inhibitor.

Electrochemical parameters obtained from polarization curves are listed in Table 1. It can be seen that as soon as the inhibitor is added, the E_{corr} value was shifted towards nobler values, except with the addition of 1.61×10^{-5} mol l^{-1}, where the E_{corr} becomes slightly more active. The I_{corr} value was calculated from the cathodic branch of polarization curve as shown on Fig. 2. Similar method has been employed by other researchers for non-Tafel dependence curves in CO_2-saturated systems [11, 20]. The I_{corr} value decreases with the addition of carboxyethyl imidazoline, reaching the lowest value with 8.1×10^{-5} mol l^{-1},

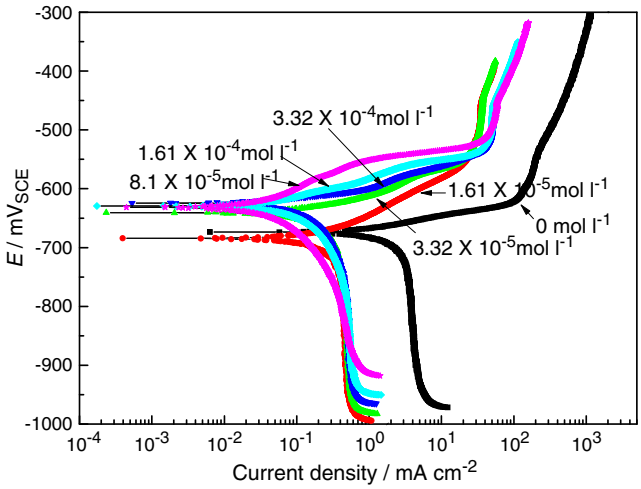

Fig. 2 Effect of carboxyamido imidazoline concentration in the polarization curves for X-70 pipeline steel in CO_2-saturated 3% NaCl solution

Table 1 Electrochemical parameters obtained from polarization curves

Inhibitor concentration (mol l^{-1})	E_{corr} (mV_{SCE})	I_{corr} (mA cm^{-2})	b_a (mV dec^{-1})	η (%)
0	−680	3.30	25	–
1.61×10^{-5}	−690	0.34	65	90
3.32×10^{-5}	−645	0.31	52	91
8.1×10^{-5}	−630	0.15	46	96
1.61×10^{-4}	−625	0.33	40	91
3.32×10^{-4}	−625	0.39	40	88

obtaining the highest inhibitor efficiency with this inhibitor concentration. On that on the anodic branch of the polarization curve, Fig. 2, an abrupt increase of the current density emerged in presence of the inhibitor when the polarization potential attains a relatively positive value, especially with 8.1×10^{-5} mol l^{-1}, which indicates an anodic desorption process of the inhibitor [11].

The increase of polarization potential accelerates the dissolution of metal not only on the surface without adsorbed species but also the surface with adsorbed inhibitive species because the adsorbed species becomes unstable at a high polarization potential. The adsorbed inhibitor species will depart metal surface quickly due to the anodic dissolution of the metal. This desorption process seems to end at a potential close to −550 mV_{SCE} regardless of the inhibitor concentration, when another abrupt in the anodic current density is observed, and an anodic limit current density was observed.

On the cathodic branch, a cathodic limiting current can be seen, which is due to the hydration of CO_2 to give carbonic acid as follows [21]:

$$CO_2 + H_2O \rightarrow H_2CO_3 \quad (4)$$

Since the solution is de-aerated, the dominant cathodic reactions are the reduction of H^+ ions, dissociation of carbonic acid [22–28]:

$$H_2CO_3 + e^- \rightarrow H^+ + HCO_3^- \quad (5)$$

$$HCO_3^- + e^- \rightarrow H^+ + CO_3^{2-} \quad (6)$$

$$2H^+ + 2e^- \rightarrow H_2 \quad (7)$$

and water reduction:

$$2H_2O + 2e^- \rightarrow 2OH^- + H_2 \quad (8)$$

The main anodic reaction, in absence of inhibitor, is iron dissolution according to:

$$Fe \rightarrow Fe^{2+} + 2e^- \quad (9)$$

though it may be through several steps. During this corrosion process, a corrosion scale of iron carbonate, $FeCO_3$, would form on the surface of carbon steels according to [29]:

$$Fe^{2+} + CO_3^{2-} \rightarrow FeCO_3 \quad (10)$$

In absence of oxygen, the primary cathodic reactions are dependent on the pH solution, and it could be the reduction of bicarbonate ions, water, and hydrogen ions (Eqs. 6–8). At a low pH value, H^+ reduction is the dominant cathodic reaction because of the high H^+ concentration. When pH increases to 4–6, as in the present case, the direct reduction of HCO_3^- and H_2CO_3 become important. At a high overpotential, the dominant cathodic reaction changes to direct reduction of water. Thus, in the present case, the diffusion of HCO_3^- and H_2CO_3 ions to from iron carbonate, $FeCO_3$, is the rate controlling step, which is independent of the inhibitor concentration, as shown in the cathodic branch of polarization curves in Fig. 2. On top of this iron carbonate film, the inhibitor-formed film is anchored to protect the metal from the electrolyte.

The effect of the carboxyamido imidazoline concentration on the change in the R_p value with time for X-70 pipeline steel exposed to a CO_2-saturated 3% NaCl solution at 50 °C is shown on Fig. 3. The inhibitive effect of carboxyamido imidazoline can be clearly seen with an increase in the R_p value with respect to the uninhibited,

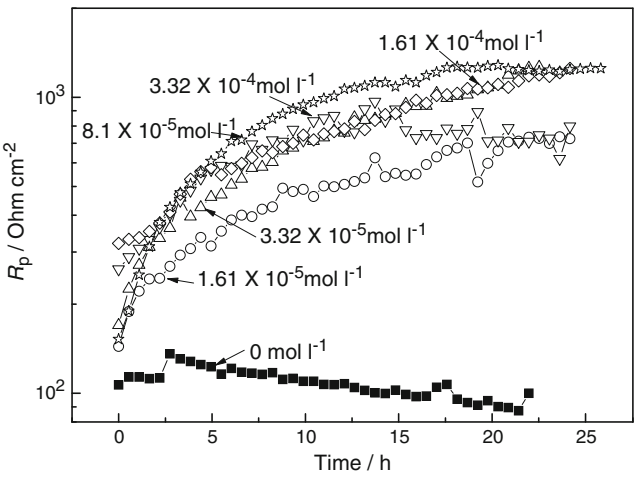

Fig. 3 Effect of carboxyamido imidazoline concentration on the change in the R_p value with time for X-70 pipeline steel in CO_2-saturated 3% NaCl solution

blank solution, for up to one order of magnitude for the addition of 8.1×10^{-5} mol l^{-1} of inhibitor. The R_p value for the blank solution decreases as time elapses, indicating an increase in the corrosion rate, which shows the non-protective nature of the corrosion products. As soon as the carboxyamido imidazoline is added, the R_p value increases with time, reaching a steady state value, regardless of the inhibitor concentration, showing a decrease in the corrosion rate and the protective nature of the film-formed inhibitor, which can be explained only with a desorption process.

Molecular structure of carboxyamido imidazoline, Fig. 1, is composed of a five-member ring containing nitrogen elements, a C-14 saturated hydrophobic head group, and a pendant, hydrophilic carboxyamido group attached to one of the nitrogen atoms. The compound can be adsorbed on the metal surface by the formation of an iron–nitrogen co-ordination bond and by a pi-electron interaction between the pi-electron in the head group and iron [11–14]. Though not a primary contribution to the adsorption strength of the compound on the surface of the metal, coulombic attraction between the negative charge, i.e. electrons, on the metal surface (as a result of the specific adsorption of chloride ions) and the imidazoline derivative may also contribute to the inhibition ability of the compound. When the adsorbed inhibitor molecules exceed certain number of atoms on the surface and these molecules are close enough, electrostatic repulsion between the negative charge of the pendant group, leads to a desorption of the inhibitor molecules, leading to unprotected sites on the metal and an increase on the corrosion rate.

Time records of current and potential for the uninhibited solution is shown on Fig. 4. This figure shows transients in current of low frequency and high intensity, with an abrupt in their intensity towards the anodic direction, and a slow decay towards the cathodic direction, typical of a material undergoing pitting corrosion [30, 31]. Simultaneously to these transients in current, there were transients in potential in the opposite direction. In both cases, there is some background noise which consists of transients with higher frequency but much lower intensity. The anodic increase in the current value indicates a rupture of the external film, whereas the slow decay in the current value indicates the rebuilding of it.

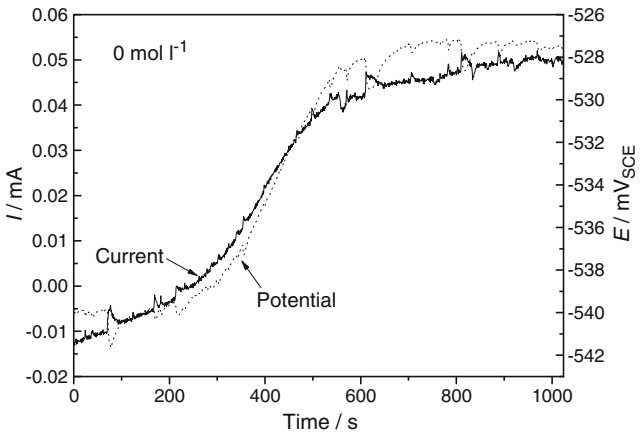

Fig. 4 Noise in current and potential for X-70 pipeline steel exposed to the uninhibited CO_2-saturated 3% NaCl solution

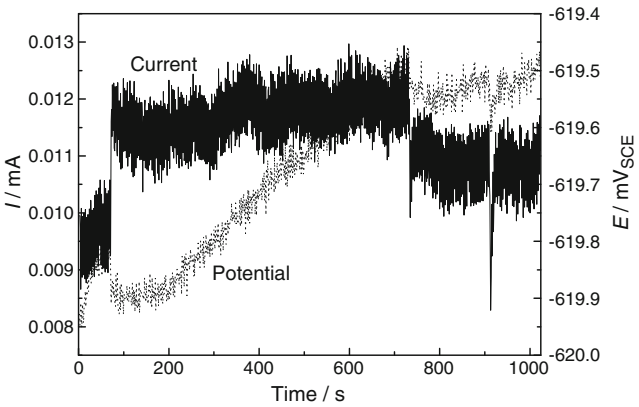

Fig. 5 Noise in current and in potential for X-70 pipeline steel exposed to the CO_2-saturated 3% NaCl solution with the addition of 8.1×10^{-5} mol l^{-1} of carboxyamido imidazoline

As stated above, in CO_2-containing solutions, the corrosion of iron and steel is controlled by the formation of an iron carbonate, $FeCO_3$ film. The increase in current shows the non-protective nature of this film. The sudden increase in the current shown by the anodic transients show that this film is being disrupted in some localized places and a localized type of corrosion such as pitting is occurring. Once this film is disrupted, this film is re-established and the noise starts to decrease, but if it is broken again, a small increase in the current with a slow recovery can be seen again. Thus, these transients indicate external film rupture-rebuilding events.

On the other hand, time series for the solution containing 8.1×10^{-5} mol l^{-1} of inhibitor, Fig. 5, showed only transients of low intensity and high frequency; it can be seen during the first seconds, the intensity of the current increases, indicating an increase of the corrosion rate but it is much smaller than that shown by uninhibited solution, Fig. 4, because the metal is covered by the inhibitor-formed film; after 200 s or so, the film is stable, and the intensity or amplitude of the current transients remain more or less constant with time, indicating the protective nature of the film-formed inhibitor. These transients are typical of a metal covered by an external protective film [30, 31] undergoing uniform corrosion, but not passivation, since polarization curves did not show the existence of a passive film.

Similar transients to these were found by Tan et al. [19], for carbon steel in a CO_2-saturated 3% NaCl solution with

20 ppm of imidazoline, with transients decreasing in intensity as time elapsed when inhibitor was present, but without inhibitor, the transients increased in intensity, thus, the corrosion rate increased in absence of inhibitor. Thus, noise transients can give us information not only about the type of corrosion that is taking place on a metal surface but also about the film formation process and its evolution with time. Additionally, noise transients can give us information about the corrosion rate as follows.

The combined effect of the ratio between the potential noise standard deviation, σ_v, over the current noise standard deviation, σ_i, after removing the trend to the times series gave a noise resistance value, R_n, and the change of this value with time for the different carboxyamido imidazoline concentrations is shown on Fig. 6. This behavior is very similar to that shown by R_p on Fig. 3: the lowest value corresponds to the uninhibited solution, but as soon as the inhibitor is added, the R_n value starts to increase in a slow fashion until it reaches a steady state value after some time.

The R_n values shown on Fig. 6 are quite similar to the R_p values shown on Fig. 3, just as found by Tan et al. [19], which confirms the similarity of noise resistance and polarization resistance, and strongly suggests a correlation of electrochemical noise with corrosion rate; this way, R_n can be used in Eq. 2 instead of R_p to calculate corrosion rates. The increase in the R_n value with time until it reaches a steady state value, and therefore a decrease in the corrosion rate as time elapses, indicates the process of formation and establishment of an inhibitor-formed film. The highest R_n value is obtained with the addition of 8.1×10^{-5} mol l^{-1}, one order of magnitude higher than the obtained for the blank solution. Lower or higher inhibitor concentrations than 8.1×10^{-5} mol l^{-1} give lower R_n values, indicating an increase in the corrosion rate.

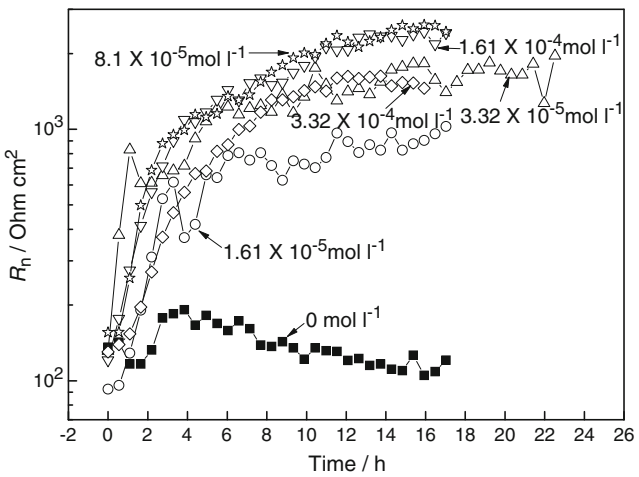

Fig. 6 Effect of carboxyamido imidazoline concentration on the change in the R_n value with time for X-70 pipeline steel in CO_2-saturated 3% NaCl solution

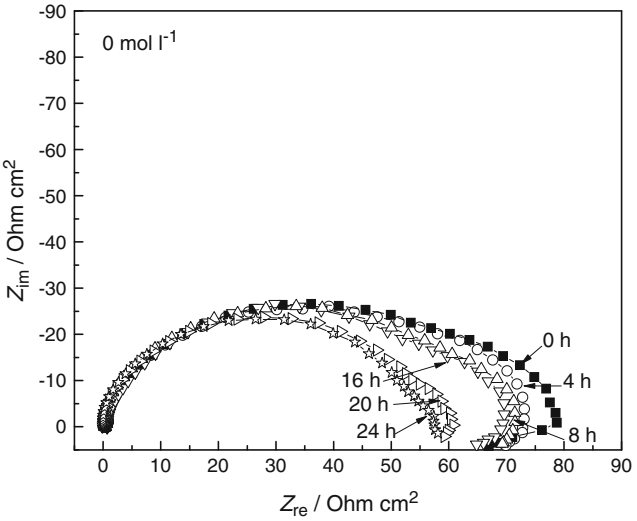

Fig. 7 Nyquist diagrams for X-70 pipeline steel in uninhibited CO_2-saturated 3% NaCl solution measured at E_{corr}

Nyquist diagram for X-70 pipeline steel exposed to a CO_2-saturated 3% NaCl solution at 50 °C is shown on Fig. 7, where it can be seen that, at high frequency values, the data describes a depressed, capacitive-like semicircle, with its center at the real axis, indicating that the corrosion process is under charge transfer control from the metal surface to the environment through the double electrochemical layer. At lower frequency values, the presence of an inductive loop is evident, which has been associated to the adsorption of intermediate species [11] and was found to be adsorbed FeOH due to the hydrolysis of Fe according to:

$$Fe + H_2O \rightarrow Fe(OH)_{ads} + e^- \quad (11)$$

$$Fe(OH)_{ads} \rightarrow FeOH^+ + e^- \quad (12)$$

$$FeOH^+ + H^+ \rightarrow Fe^{2+} + H_2O \quad (13)$$

The high-frequency semicircle diameter corresponds to the charge transfer resistance, R_{ct}, equivalent to the polarization resistance, R_p, thus inversely proportional to the corrosion current density, I_{corr} in Eq. 2

As time elapses, the high-frequency semicircle diameter decreases, increasing, thus, the corrosion rate, showing the non-protective nature of the corrosion products. CO_2 corrosion of carbon and low alloy steels is strongly dependent on the surface formed films during the corrosion processes. The protectiveness, rate of formation/precipitation, and the stability of the film controls the corrosion rate and its nature. The main formed film during CO_2 corrosion of iron and low alloy steels is iron carbonate, $FeCO_3$, which is affected by iron and carbonate concentrations and

temperature. All authors agree that increasing the temperature would improve the protectiveness of the $FeCO_3$ scales as well as its adherence and hardness [21–27, 32]. The lowest temperature necessary to obtain $FeCO_3$ films that would reduce the corrosion rate is 50 °C.

When 1.61 or 3.23×10^{-5} mol/l of carboxyamido imidazoline is added to the solution, Nyquist diagrams show similar features to those for uninhibited solution, Fig. 8, with a capacitive semicircle at high-frequency values, followed by an inductive loop at lower frequencies. However, when 8.1×10^{-5} mol l^{-1} of carboxyamido imidazoline are added, Fig. 9, the data describes a straight line at high-frequency values followed by a capacitive-like semicircle at lower frequencies during the first 8 h approximately. After this time, the data describes a single, capacitive semicircle. For the data obtained during the first 8 h, the straight line and semicircle indicates that the corrosion process is under diffusion and charge transfer mixed control. This is due to the diffusion of aggressive species through the inhibitor-formed film. On the other side, for times longer than 8 h, the semicircle shows that the corrosion mechanism is under charge transfer control only. The semicircle diameter was almost three orders of magnitude bigger than that obtained for lower carboxyamido imidazoline concentrations.

For inhibitor concentrations higher than 8.1×10^{-5} mol l^{-1}, Fig. 10, the corrosion process is under a diffusion and charge transfer mixed controlled mechanism during the first hours, but after 4 h approximately, the data describes a depressed, capacitive semicircle, with a diameter much smaller than that obtained with 8.1×10^{-5} mol l^{-1} of carboxyamido imidazoline, within the same order of magnitude than those obtained with inhibitor concentrations lower than this one. The

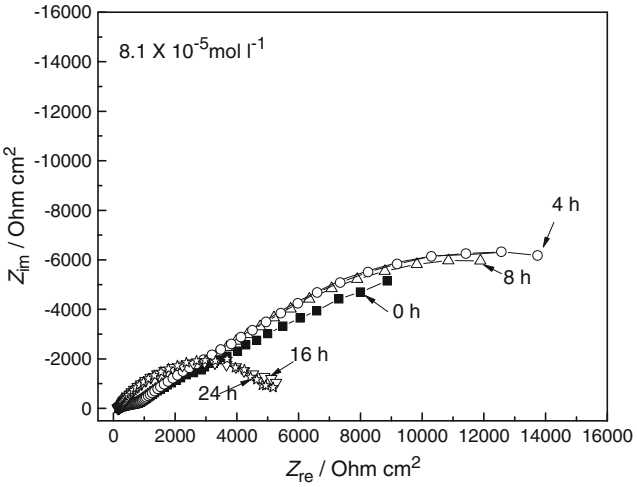

Fig. 9 Nyquist diagrams for X-70 pipeline steel in CO_2-saturated 3% NaCl solution containing 8.1×10^{-5} mol l^{-1} of carboxyamido imidazoline measured at E_{corr}

corrosion mechanism for times longer than 4 h is under charge transfer control. Thus, we can see that an adsorption controlled mechanism is found for carboxyamido imidazoline concentrations than 8.1×10^{-5} mol l^{-1}; for carboxyamido imidazoline concentrations equal to 8.1×10^{-5} mol l^{-1}, the corrosion mechanism is under diffusion and charge transfer mixed control, whereas for carboxyamido imidazoline concentrations higher than 8.1×10^{-5} mol l^{-1}, the corrosion mechanism is under charge transfer control.

It can be noticed that the inhibitor behaves in different ways during the first hours of testing depending upon its concentrations. At low concentration, Fig. 8, there is a depressed, capacitive-like semicircle at high and intermediate frequency values, indicating that the corrosion process

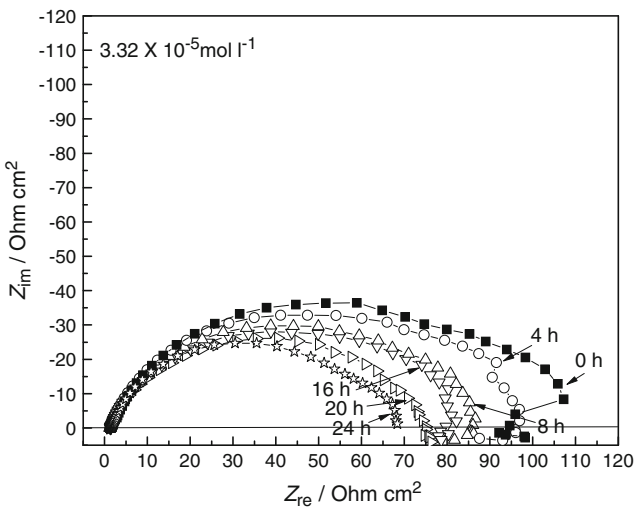

Fig. 8 Nyquist diagrams for X-70 pipeline steel in CO_2-saturated 3% NaCl containing 3.32×10^{-5} mol l^{-1} of carboxyamido imidazoline solution measured at E_{corr}

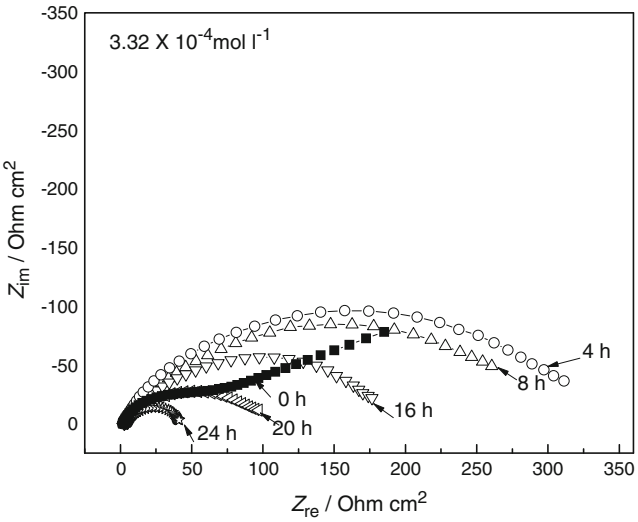

Fig. 10 Nyquist diagrams for X-70 pipeline steel in CO_2-saturated 3% NaCl solution containing 3.32×10^{-4} mol l^{-1} of carboxyamido imidazoline measured at E_{corr}

is under charge transfer control from the metal surface to the environment through the double electrochemical layer. At lower frequency values, the presence of an inductive loop is evident, which has been associated to the adsorption of intermediate species. At intermediate inhibitor concentrations, Fig. 9, data described a straight line followed by a semicircle at low frequencies, indicating a finite type of diffusion coupled to a charge transfer mechanism, charge transfer from the alloy to the electrolyte. However, at high inhibitor concentrations, Fig. 10, at the beginning of the experiment data describe a semicircle at high frequency values followed by a straight line, indicating a type of infinite diffusion of aggressive ions; this time, the diffusion of aggressive ions is from the bulk solution to the metal, dislike at intermediate inhibitor concentrations, where there was a finite diffusion through the film-formed inhibitor. In any case, the slow diffusion of aggressive ions is the rate controlling process, decreasing, this way, the corrosion rate of steel in presence of inhibitor.

Conclusions

A study on the effect of carboxyamido imidazoline concentration on the CO_2 corrosion of X-70 steel by using different electrochemical techniques has been carried out. Different techniques have shown good inhibition properties of carboxyamido imidazoline in salt water saturated with CO_2, which increased with its concentration, reaching the highest corrosion protection with 8.1×10^{-5} mol l^{-1}. Lower or higher carboxyamido imidazoline concentrations than 8.1×10^{-5} mol l^{-1} increases the corrosion rate because the surface area covered by the inhibitor decreases. A mechanism has been used to explain the inhibitor desorption for concentration higher than the most efficient one. EN measurements can give information not only about the type of corrosion that is taking place on a metal surface, but also about the film formation process and its evolution with time. Additionally, there was a corrosion mechanism different for inhibitor concentrations lower than 8.1×10^{-5} mol l^{-1}, a different one for this concentration, and another one for concentrations higher than 8.1×10^{-5} mol l^{-1}. Carboxyamido imidazoline was a kind of anodic inhibitor.

Acknowledgments D. M. Ortega and A. Caceres acknowledge CONACYT – MEXICO for the support of a graduate scholarship to CIMAV and FQ-UNAM. Corrosion y Proteccion Ingeniería SC and ICF-UNAM acknowledge the support of grant FOMIX MOR-2008-C01-93689.

References

1. Nesic S (2003) Corrosion 59:616–629
2. Song M, Kirk DW, Graydon JW, Cormarck DE (2004) Corrosion 60:736–740
3. Kermani MB, Harrop D (1996) J SPE Production Facilities 8:186–197
4. Kermani MB (2000) NACE paper No. 156, NACE, Houston
5. McIntyre P (2002) Corrosion Management 46:19–25
6. Kermani MB, Harrop D (1993) Materials Selection for Oil and Gas Productionand Transportation Facilities. Third International Corrosion Congress, Tehran
7. Rodriguez-Valdez LM, Villamisar W, Casales M, Gonzalez-Rodriguez JG, Martinez-Villafañe A, Martinez L, Glossman-Mitnik D (2006) Corros Sci 48:4053–4064
8. Liu X, Okafor PC, Zheng YG (2009) Corros Sci 51:744–751
9. Okafor PC, Liu X, Zheng YG (2009) Corros Sci 51:761–768
10. Liu FG, Du M, Zhang J, Qiu M (2009) Corros Sci 51:102–109
11. Zhang GA, Cheng YF (2009) Corros Sci 51:87–94
12. Liu X, Zheng YG (2008) Corros Eng, Sci Technol 43:87–92
13. Zhao JM, Lu Y, Liu HX (2008) Corrosion Eng Sci Tech 43:313–319
14. Okafor PC, Nesic SI (2007) Chem Eng Commun 194:141–149
15. Durnie W, Kinsella B, De Marco R, Jefferson A (2001) J Appl Electrochem 31:1221–1229
16. Farelas F, Galicia M, Brown B, Nesic S, Castaneda H (2010) Corros Sci 52:509–522
17. Garcia-Ochoa E, Genesca J (2004) Surf Coat Technol 184:322–330
18. Malo JM, Uruchurtu J, Corona O (2002) Corrosion 58:932
19. Tan YJ, Bailey S, Kinsella B (1996) Corros Sci 38:1681–1695
20. Reznik VS, Akamsin VD, Khodyrev YP, Galiakberov RM, Efremov YY, Tiwari L (2008) Corros Sci 50:392–403
21. Nesic S, Postlehwaite J, Olsen S (1996) Corrosion 52:280–296
22. De Waard C, Milliams DE (1975) Corrosion 31:131–136
23. Schmitt G, Rothman B (1977) Werkst Korros 28:816–825
24. Hurlen T, Gunvaldsen S, Tunold R, Blaker F, Lunde PG (1984) J Electroanal Chem 180:511–519
25. Gray LGS, Anderson BG, Danysh MJ, Tremaine PG (1989) NACE paper No. 464, NACE Houston
26. Gray LGS, Anderson BG, Danysh MJ, Tremaine PG (1989) NACE paper No. 40, NACE, Houston
27. Bonis MR, Crolet JL (1989) NACE paper No. 466, NACE, Houston
28. Mora-Mendoza JL, Turgoose S (2001) NACE paper No. 63, NACE, Houston
29. Lopez DA, Schreiner WH, de Sanchez SR, Simison SN (2003) Appl Surf Sci 207:69–76
30. Hladky K, Dawson JL (1982) Corros Sci 22:231–237
31. Dawson JL, Rothwell AN, Walsh TG, Lawson K, Palmer JW (1993) NACE paper No. 108, NACE, Houston
32. Walter GW (1986) Corros Sci 26:681–703